

Original Paper

Annexin A2-S100A10 Represents the Regulatory Component of Maxi-Cl Channel Dependent on Protein Tyrosine Dephosphorylation and Intracellular Ca²⁺

Md. Rafiqul Islam^a Toshiaki Okada^a Petr G. Merzlyak^{a,b} Abduqodir H. Toychiev^{a,c}
Yuhko Ando-Akatsuka^d Ravshan Z. Sabirov^{a,b} Yasunobu Okada^{a,e}

^aDivision of Cell Signaling, National Institute for Physiological Sciences (NIPS), Okazaki, Japan, ^bInstitute of Biophysics and Biochemistry, National University of Uzbekistan, Tashkent, Uzbekistan, ^cDepartment of Biological Sciences, State University of New York College of Optometry, New York, NY, USA, ^dDepartment of Cell Physiology, Faculty of Pharmaceutical Sciences, Suzuka University of Medical Science, Suzuka, Japan, ^eDepartment of Physiology, Kyoto Prefectural University of Medicine, Kyoto, Japan

Key Words

Annexin A2-S100A10 • Ca²⁺ • Maxi-Cl channel • Protein tyrosine dephosphorylation • SLCO2A1

Abstract

Background/Aims: Maxi-anion channel (Maxi-Cl) is ubiquitously expressed and involved in a number of important cell functions especially by serving as an ATP release pathway. We recently identified SLCO2A1 as its essential core component. However, the regulatory component required for the channel activation/inactivation remains unidentified. **Methods:** In the present study, to identify the regulatory component, we made genome-wide analysis combined with siRNA screening and performed patch-clamp studies and ATP release assay after gene silencing and overexpression. **Results:** Comparative microarray analysis between Maxi-Cl-rich C127 and -deficient C1300 cells revealed highly differential expression not only of SLCO2A1 but also of four annexin family members. Gene silencing study showed that *Anxa2* is involved in Maxi-Cl activity. The Maxi-Cl events appeared in C1300 cells by overexpression of *Slco2a1* and more efficiently by that of *Slco2a1* plus *Anxa2*. Immunoprecipitation assay supported the interaction between ANXA2 and SLCO2A1. Suppressing effects of overexpression of a phospho-mimicking mutant of *Anxa2*, *Anxa2*-Y23E, indicated that protein tyrosine dephosphorylation dependence of Maxi-Cl is conferred by ANXA2. Maxi-Cl activity was suppressed by gene silencing of S100A10, a binding partner of ANXA2, and by applying a synthetic ANXA2 peptide, Ac-(1-14), which interferes with the ANXA2-S100A10 complex formation. Intracellular Ca²⁺ dependence of Maxi-Cl activity was abolished by *S100a10* knockdown.

M. R. Islam and T. Okada contributed equally to this work.

Yasunobu Okada, MD, PhD

National Institute for Physiological Sciences
Higashiyama 5-1, Myodaiji-cho, Okazaki 444-8787 (Japan)
Tel. +81-564-59-5262, Fax +81-564-59-5263, E-Mail okada@nips.ac.jp

Conclusion: The ANXA2-S100A10 complex represents the regulatory component of Maxi-Cl conferring protein tyrosine dephosphorylation dependence and intracellular Ca^{2+} sensitivity on this channel.

© 2020 The Author(s). Published by
Cell Physiol Biochem Press GmbH&Co. KG

Introduction

A major type of large-conductance anion channel, Maxi-Cl, is ubiquitously expressed and is phenotypically characterized by a large unitary conductance (300-500 pS), a linear I - V relationship, time-dependent inactivation at both positive and negative potentials (usually over ± 20 mV), high anion selectivity ($P_{\text{Cl}}/P_{\text{Na}}$ of >6) and a bell-shaped P_o - V relationship [for reviews see [1, 2]]. Maxi-Cl plays important roles in many physiological and pathophysiological cell functions, including the tubulo-glomerular feedback in kidney, ischemia and hypoxia injury in heart and brain, and excitotoxic neurodegeneration [for reviews see [1, 3]] as well as in absorption of free fatty acid in colonic epithelial cells [4, 5]. Maxi-Cl channel serves as a very efficient pathway for releasing ATP [6, 7]. By applying proteomics and unbiased genome-wide approaches, recently, *SLCO2A1* was identified as the core (or pore) component of Maxi-Cl [8]. Maxi-Cl is non-activated in intact cells in the basal state, and therefore the channel event is not observed in the patch membrane under the cell-attached or on-cell configuration without any stimulation [for review see [9]]. In contrast, Maxi-Cl channels reconstituted with recombinant *SLCO2A1* proteins were found to be constitutively activated [8], the fact indicating that the whole Maxi-Cl complex contains not only the core component, *SLCO2A1*, but also some regulatory component(s) involved in the channel activation/inactivation mechanism. So far, on-cell Maxi-Cl activity has been shown to be provoked not only by osmotic cell swelling [for reviews see [1, 2]], which ordinarily provokes a rise in the intracellular free Ca^{2+} concentration [for review see [10]], or by application of a Ca^{2+} ionophore A23187 [11-15] but also by application of protein tyrosine kinase blockers [16, 17]. Thus, it is strongly suggested that some Ca^{2+} -dependent protein susceptible to protein tyrosine kinase/phosphatase represents the regulatory component for Maxi-Cl. In addition, Maxi-Cl activity was found to be constitutively activated in the patch membrane on the blebs that emerged from mouse C127 cells treated with an actin polymerization inhibitor latrunculin B [8]. Thus, it is likely that the regulatory component for Maxi-Cl is some actin-related protein.

To identify the regulatory component, presumably an actin-related, Ca^{2+} -dependent and tyrosine residue-containing protein, in the present study, genome-wide analysis combined with siRNA screening was performed between a Maxi-Cl-rich mouse C127 cell line and a Maxi-Cl-deficient mouse C1300 cell line. The present results demonstrated that both a member of annexin family, annexin A2 (ANXA2), Tyr23 of which can be phosphorylated/dephosphorylated, and its binding partner Ca^{2+} -binding protein, S100A10, are essentially involved in the regulation of Maxi-Cl channels. Thus, it is concluded that the ANXA2-S100A10 complex, which is known to bind to and interact with filamentous F-actin [18-20], plays regulatory roles for the Maxi-Cl/*SLCO2A1* channel activity by conferring tyrosine dephosphorylation dependence and intracellular Ca^{2+} sensitivity on this channel.

Materials and Methods

Cell culture

A fibroblastic cell line of mouse mammary tissue origin, C127, obtained from the American Type Culture Collection was cultured in Dulbecco's modified Eagle's medium (DMEM) supplemented with 200 mg/L penicillin (Meiji Seika, Tokyo, Japan), 100 mg/L streptomycin (Meiji Seika) and 10% fetal bovine serum (FBS) (PAA Laboratories, Pasching, Austria). Mouse neuroblastoma C1300 cells obtained from RIKEN BRC (Tsukuba, Japan) were grown in DMEM supplemented with 5% FBS (PAA Laboratories, Yeovil, UK). Human embryonic kidney HEK293T cells were grown in DMEM supplemented with 10% FBS (Biowest, Nuaille, France). Cells were maintained at 37°C in a 5% CO_2 incubator and were usually split every 3-4 days. For

patch-clamp experiments, cells were grown on glass coverslips and were transferred to the bath chamber immediately before experiments.

Microarray analysis

Microarray analysis was carried out with Affymetrix GeneChip® Mouse Gene 1.0 ST Arrays (Affymetrix Inc., Santa Clara, CA, USA) according to the standard Affymetrix protocol. Total RNAs were extracted from C127 and C1300 cells using SEPASOL (Nacalai Tesque, Kyoto, Japan), purified with the RNeasy® Minikit (Qiagen, Hilden, Germany) and processed to cDNA (target) using the Ambion® WT Expression Kit (Thermo Fisher Scientific) and the GeneChip® WT Terminal Labeling and Controls Kit (Affymetrix Inc.). The raw CEL files were processed for gene-level analysis with median polish summarization and quantile normalization using Affymetrix® Expression Console™ 1.1 software (Affymetrix Inc.), and normalized intensity values were obtained. To identify up- or down-regulated genes, we calculated the ratio (non-log scaled fold-change) from the normalized intensity of each gene for comparisons between C1300 and C127 cells. Since an Affymetrix average difference (AD) level of 100 is thought to correspond to an extremely low or zero level of expression, we only took genes for which there was an AD value greater than 100 into consideration. Microarray analysis support was provided by Cell Innovator (Fukuoka, Japan).

siRNA-mediated transient knockdown

To test the effects of transient knockdown of *Anxa2* and *S100a10* on Maxi-Cl channel activity, one-day cultured C127 cells sparsely seeded on 24-well plates were transfected with siRNAs against mouse *Anxa2* (ID: Stealth siRNA MSS273457, Thermo Fisher Scientific, Waltham, MA, USA) and mouse *S100a10* (ID: Stealth siRNA MSS276910, Thermo Fisher Scientific) at a concentration of 20–25 nM using HiPerFect transfection reagent (Qiagen) with serum-free OPTI-MEM (Thermo Fisher Scientific) according to the manufacturer's manual. To test the effects of transient knockdown of *Anxa1*, *Anxa3*, *Anxa6* and *Anxa11* expression on Maxi-Cl channel activity, C127 cells were transfected with following siRNAs against mouse annexin members: *Anxa1* (ID: S100194908, Qiagen, Hilden, Germany), *Anxa3* (ID: Mm01_00169933, Qiagen), *Anxa6* (ID: 1322252, Bioneer, CA, USA) and *Anxa11* (ID: S100898975, Qiagen). One day after transfection, the cells were washed with culture medium and grown in the same medium for one additional day at 37°C before use for RT-PCR, western blotting, ATP release assay or patch-clamp experiments. Stealth RNAi™ siRNA Negative Control (Thermo Fisher Scientific) was also transfected into C127 cells as the mock control.

Validation of siRNA efficacy

Molecular expression of the targeted genes and their knockdown by gene-specific siRNAs were monitored by RT-PCR. Total RNA was isolated from cultured cells using Sepasol RNA I reagent (Nacalai Tesque, Kyoto, Japan) according to the manufacturer's instructions. Total RNA was treated with DNase I (Takara Bio Inc., Otsu, Japan) to remove genomic DNA. cDNA was synthesized using an oligo-dT primer (Thermo Fisher Scientific) and PrimeScript II 1st-Strand cDNA Synthesis Kit (Takara Bio Inc.). To amplify the *Anxa2* and *S100a10* fragments, primer sets (forward: 5'- tgggccagtcgcatccagaac -3', reverse: 5'- ctctagaacccag-gttggg -3', product size 309 bp; and forward: 5'-tgagagtgtcatggaacgg -3' reverse: 5'-attcctcaagtgaccccggtg -3' product size 266 bp, respectively) were used. *Gapdh* was also amplified as an internal control (forward: 5'-gcacagtcaaggccgagaat-3', reverse: 5'-ttcaccaccatggagaaggc-3', product size 151 bp). To amplify the *Anxa1*, *Anxa3*, *Anxa6* and *Anxa11* fragments, the following primer sets were used: for *Anxa1* (forward: 5'- tctgag-cagagtctctcttcagtc -3' , reverse: 5'- tgaagtacgaggccttgatctg -3' , product size 331 bp), *Anxa3* (forward: 5'-aggacttgggactgacgaga -3' , reverse: 5'- aggcctgagattctctc -3' , product size 299 bp), *Anxa6* (forward: 5'-cagaugaaaagacucucau -3' , reverse: 5'- augagagucuuuucacug -3' , product size 292 bp) and *Anxa11* (forward: 5'- agagcacactctcggtttccc -3' , reverse: 5'- cactctcccacaacacga -3' , product size 362 bp).

The effect of siRNA against *Anxa2* was also assessed at the protein expression level by western blotting. Total proteins of C127 cells transfected with *Anxa2*-specific siRNA or non-targeting siRNA were isolated using RIPA buffer (Chromo Tec, Hauppauge, NY, USA). Solutions containing the proteins were boiled in Tris-Glycine SDS sample buffer (2x) (Thermo Fisher Scientific) at 95°C for 5 min. Five to 10 µL of samples were loaded on to a 12% precast gel (Mini-protean® TGX™: BIO-RAD, Hercules, CA, USA) and transferred to a nitrocellulose membrane using iBlot blotting system (Thermo Fisher Scientific). ANXA2 proteins were then detected with anti-ANXA2 antibody (No. 610069: BD Biosciences, San Jose, CA, USA) (1:1000) in TBS and ECL™ Prime Western Blotting Detection Reagent (Amersham™/GE Healthcare, Buckinghamshire, UK). After

signal detection, membranes were treated with 15% H₂O₂ in PBS to inactivate HRP. Then, beta actin was detected on the same membrane using polyclonal antibody (Cat. No. GTX109639: GENE TEX, Inc., Irvine, CA, USA) as the internal control.

miRNA-mediated stable Anxa2 knockdown

To generate a stable *Anxa2* knockdown cell line, we adopted BLOCK-iTTM Pol II miR RNAi Expression Vector System (Thermo Fisher Scientific), as previously described [8]. Briefly, Pre-miRNA double stranded DNA oligo against *Anxa2* (oligo ID, *Mmi505548*: Thermo Fisher Scientific) was inserted into pcDNATM6.2-GW/EmGFP-miR vector. The miR-neg control plasmid included in the kit was used as a negative control. Vectors against *Anxa2* or negative control were transfected into C127 cells. Transfected cells were cultured in the medium containing 25–50 µg/mL of blasticidin (Thermo Fisher Scientific). About four weeks later, GFP-positive colonies were cloned.

Gene cloning and overexpression study

The full length coding sequence of *Anxa2* with Kozak translation initiation sequence was amplified from cDNAs of murine C127 cells by using a gene-specific PCR primer set (forward: 5'- cacaacctgtctactgtccacg -3', reverse: 5'- tgtgctgagccttcagtcac -3'), and the amplified PCR product was cloned into pGEM-T easy vector. To produce the expression vectors for mammalian cell lines, the wild-type of *Anxa2* was then subcloned into a bicistronic vector (CMV-pIRES2-dsRED2: Clontech, Mountain View, CA, USA). *Anxa2*-Y23E expression vector and dsRED2-tagged-*Anxa2* protein expression vector were generated by PCR-based mutagenesis using the following primer sets (forward: 5'- gggctagcacaacctacaccaactcg -3', reverse: 5'- ctcgcaactgggggttagaatgac -3'; and forward: 5'- atggcctctccgagaacgac -3', reverse: 5'- gtcacccccaccacagga -3', respectively). The expression vectors were transfected into C1300 or C127 cells using Lipofectamine 3000 Transfection Reagent (Invitrogen, Thermo Fisher Scientific) according to the manufacturer's instructions. Transfected cells were provided for inside-out mode patch-clamp, coimmunoprecipitation and immunocytochemistry experiments within a period of 48 h after transfection. CMV-pIRES2-dsRED2 or -EGFP empty vector was used for mock transfection control. *Slco2a1*-ires-EGFP vector, EGFP-tagged-*Slco2a1* protein expression vector and *Slco2a1*-FLAG sequence (DYKDDDDK)-tagged vector were used for overexpression studies, as used in our previous study [8].

Coimmunoprecipitation

To prepare membrane fractions, HEK293T cells co-transfected with *Slco2a1*-FLAG and CMV-*Anxa2*-DsRed2 or with *Slco2a1*-EGFP and CMV-*Anxa2*-DsRed2, were collected and washed with PBS. After centrifugation, they were suspended and kept in PBS for 30 min. Then, these cells were homogenized on ice in the presence of Complete EDTA-free Protease Inhibitor Cocktail (PIC: Merck Life Science, Darmstadt, Germany) for 1 min using a potter homogenizer. The homogenate was centrifuged (2,000 rpm for 30 min), and the post-nuclear supernatant was ultracentrifuged at 100,000×g for 30 min. After that, the high-speed pellet was suspended overnight in 400 µL of radioimmunoprecipitation assay buffer (RIPA), which contained 0.1% sodium dodecyl sulfate (SDS), 0.5% sodium deoxycholate, 1% nonidet P-40 (NP-40), 150 mM NaCl and 50 mM Tris-HCl (pH 7.5). This membrane fraction was pre-incubated with 30-µL bed volume of rec-protein A-Sepharose 4B (Invitrogen, Thermo Fisher Scientific) along with mouse IgG (Sigma-Aldrich, St. Louis, MO, USA) for 1 h at room temperature. After centrifugation, the supernatant was divided into two fractions. The one was incubated with 40-µL bed volume of rec-protein A-Sepharose 4B along with mouse IgG, and the other was incubated with 40-µL bed volume of anti-FLAG M2 affinity gel (Sigma) or 40-µL bed volume of rec-protein A-Sepharose 4B along with anti-ANXA2 monoclonal antibody (C-10: Santa Cruz Biotechnology Inc., Dallas, TX, USA). After the incubation for 2 h at room temperature, the beads were washed, and immunoprecipitates were eluted by boiling them in SDS-PAGE sample buffer. For western blotting, the proteins were electrophoresed and electrophoretically transferred onto PVDF membranes. After blocking with 5% powdered milk dissolved in Tris-buffered saline solution, which contained (in mM) 137 NaCl, 2.7 KCl, and 25 Tris-HCl (pH 7.5), supplemented with 0.1% Tween 20 (TBST), for 30 min, the membranes were incubated with the primary antibody, anti-RFP or anti-GFP polyclonal antibody (PM005 or 598: MBL, Nagoya, Japan). Bound antibodies were detected with HRP-conjugated secondary antibody using the ECL detection kit (GE Healthcare Life Sciences, Chicago, IL, USA).

Immunocytochemistry

To observe localization of SLC02A1, EGFP-tagged-*Slco2a1* protein expression vector was transfected to C127 cells. Two days after transfection, the cells were fixed with 4% formaldehyde in PBS. Cells were treated with 0.25% Triton-X in PBS for 10 min and blocked using 5% dry non-fat milk in PBS for 30 min. Then cells were incubated with anti-ANXA2 monoclonal antibody (C-10: Santa Cruz Biotechnology Inc.) diluted at 1:100 in PBS at 4°C overnight. Alexa 594-conjugated secondary antibody (goat anti-mouse IgG (H+L): Thermo Fisher Scientific) was used at 1:400. Subcellular localization of EGFP-tagged SLC02A1 and Alexa 594 associated with ANXA2 was observed using an epifluorescence microscope (IX70: Olympus, Tokyo, Japan).

Electrophysiology

All patch-clamp recordings were performed in the inside-out mode at room temperature (23–25°C), as described previously [17]. Patch pipettes were pulled from borosilicate glass capillaries (outer diameter 1.4 mm, inner diameter 1.0 mm) with a micropipette puller (Model P-97: Sutter Instruments, Novato, CA, USA) and had a tip resistance of 2 to 3 MΩ when filled with the pipette solution. Osmolality of experimental solutions was measured with a vapor pressure osmometer VAPOR 5600 (WESCOR, South Logan, UT, USA). For measurements of Maxi-Cl currents in excised patches, patch pipettes were filled with standard Ringer solution containing (in mM): 135 NaCl, 5 KCl, 2 CaCl₂, 1 MgCl₂, 5 Na-HEPES, 6 HEPES and 5 glucose (pH 7.4, 290 mOsm/kg-H₂O). Most experiments were performed by exposing the cells to standard Ringer solution. To observe the effects of changes in the intracellular free Ca²⁺ level, the excised patch membranes were exposed to artificial intracellular solutions (AISOs) containing (in mM): 140 KCl, 5 EGTA and 5 HEPES together with varying concentrations of CaCl₂. In some experiments, bath Ringer solution was supplemented with purified mouse anti-ANXA2 monoclonal antibody (No. 610069: BD Biosciences) or the control mouse IgG. When necessary, pipette and/or bath solutions were/was supplemented with a synthetic ANXA2 peptide, Ac-(1-14), the sequence of which is acetyl-STVHEILCKLSLEG (Biologica, Nagoya, Japan), or its negative control peptide, L7E-Ac-(1-14), the sequence of which is acetyl-STVHEIECKLSLEG (Biologica). For patch-clamping, the cells were plated on glass coverslips in 20–50% confluence and bathed in standard Ringer solution. Membrane currents were measured with an Axopatch 200A patch-clamp amplifier coupled to a DigiData 1320 interface (Axon Instruments, Union City, CA, USA) or with an EPC-9 patch-clamp system (Heka-Electronics, Lambrecht/Pfalz, Germany). The time course of current change was monitored by repetitively applying (every 5 s) alternating step pulses (500-ms duration) to ±25 mV from a holding potential of 0 mV. To observe voltage dependence of the current profile, step pulses were applied with command voltages up to ±50 mV in 10-mV increments. Data acquisition and analysis were done using pCLAMP software (version 9.0.2: Axon Instruments) and WinASCD software (kindly provided by Dr. G. Droogmans, Katholieke Universiteit Leuven, Belgium) or with Pulse+PulseFit (Heka-Electronics). Current signals were filtered at 2 kHz and digitized at 5 kHz.

Luciferin-luciferase ATP assay

For the ATP-release assay, we used isotonic and hypotonic 50-mM NaCl Ringer solutions containing (in mM): 50 NaCl, 5 KCl, 2 CaCl₂, 1 MgCl₂, 5 Na-HEPES, and 6 HEPES (pH 7.4; 290 and 124 mOsm/kg-H₂O, respectively, adjusted with mannitol). In these 50-mM NaCl solutions, only the amount of mannitol was varied with keeping the ionic strength at a constant level, thereby enabling reproducible ATP measurements. Hypotonicity-induced ATP release was quantified by a luciferin-luciferase assay system (ATP Luminescence Kit AF-2L1: DKK-TOA, Tokyo, Japan), as described previously [8, 21]. Briefly, the cells were cultured to confluence in 24-well plates. After fully replacing the culture medium with isotonic 50-mM NaCl Ringer solution (500 μL/well), the cells were incubated at 37°C for 60 min. A hypoosmotic challenge was then initiated by gently removing most of the extracellular solution, adding hypotonic 50-mM NaCl Ringer solution (425 μL/well), and maintaining the plates at 37°C. After 30 min of incubation, the plates were carefully rocked to ensure homogeneity of the extracellular solution, and samples (50 μL) were collected from each well for the luminometric ATP assay. After adding 500 μL H₂O and 50 μL of the luciferin-luciferase reagent, the ATP concentration in the samples, all of equal ionic strength, was measured with an ATP analyzer (Model AF-100: DKK-TOA). The assay was calibrated using a standard 100-nM ATP solution. ATP release from the cells transfected with siRNA was also similarly measured. After the luminescence measurements, the cells were trypsinized, detached by thorough pipetting, and counted manually in a cell counting chamber. The total luminescence intensity for each well was normalized by the cell number in order to assess the variability in growth rate after siRNA treatment.

Data analysis

After subtracting the background currents, the mean patch currents were measured at the beginning (first 25–30 ms) of current responses to voltage steps in order to minimize the contributions of voltage-dependent current inactivation and the channel occupancy in the sub-conductance states. The mean number of channels open, nP_o (where P_o and n represent the open channel probability and the number of active channels, respectively), was calculated by dividing the mean macro-patch current by the single-channel amplitude.

Data were analyzed in OriginPro 7 or 8.6 (Origin Lab Corporation, Northampton, MA, USA). Plotted data are given as means \pm SEM of n observations. Statistical differences of the data were evaluated by ANOVA and the paired or unpaired Student's t test where appropriate and considered significant at $p < 0.05$.

Results

SLCO2A1 and four annexin members are less prominently expressed in Maxi-Cl-deficient C1300 cells compared to those in Maxi-Cl-rich C127 cells

First, we searched for a mouse cell line lacking Maxi-Cl activity among a number of our frozen cell lines in stock and found that mouse neuroblastoma C1300 cells do not express notable channel activity. As shown in Fig. 1A and summarized in Fig. 1B, mouse mammary C127 cells displayed up to 10–15 single channels in an excised inside-out patch obtained using a 2 M Ω -pipette (A, top trace), whereas C1300 cells exhibited no channels under the same experimental conditions (A, middle trace). Although large-conductance anion channel events were previously reported to be provoked in C1300 cells after stimulation with tamoxifen [22], we failed to detect any anion channel events even ≥ 10 min after treating our C1300 cells with 10 μ M tamoxifen added to the bath and pipette solutions (Fig. 1A, bottom trace).

We then made a genome-wide microarray analysis between the mRNAs isolated from C127 and C1300 cells to select membrane proteins that are highly expressed in the former, but not latter, cell line and therefore may serve as the molecular candidates involved in Maxi-Cl activity. This analysis yielded a total of 686 genes encoding potential membrane-spanning or -associated proteins (Supplementary Table 1 – for all supplemental material see www.cellphysiolbiochem.com), that were differentially less expressed in C1300 cells compared to C127 cells with a signal ratio of higher than two (non-log-scaled fold-change). Among 15 genes encoding multiple membrane-spanning proteins that were previously found to be expressed in the Maxi-Cl-accumulated bleb membrane of C127 cells by a nano-LC-MS/MS analysis [8], *Slc33a1*, *Slc44a2*, *Slco2a1* and *Tmem62* showed differential expression with the C127/C1300 signal ratio of higher than two, and *SLCO2A1* was found to show the highest signal ratio of 17.8 (Table 1), in-

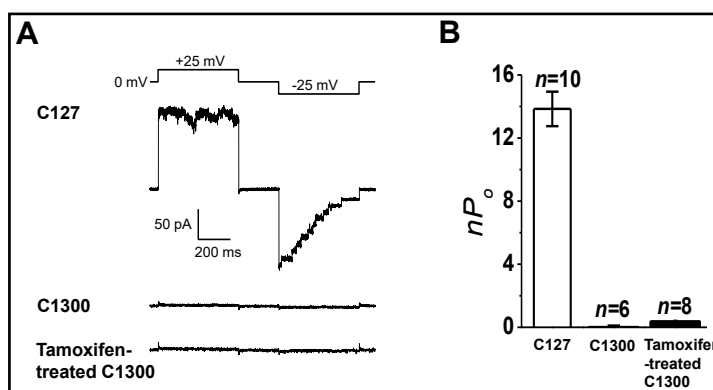


Fig. 1. Differential expression of Maxi-Cl channel activity between mouse mammary C127 cells and neuroblastoma C1300 cells. A. Maxi-Cl currents recorded in excised inside-out patches from C127 cells, but not from C1300 cells, upon application of an alternating pulse from 0 to ± 25 mV (protocol is shown at the top of the traces). In C1300 cells, even after treatment with 10 μ M tamoxifen (≥ 10 min) added to the bath (intracellular) and the pipette (extracellular) solution to mimic conditions previously reported to activate large-conductance anion channel currents in C1300 cells [22]. B. Mean patch currents recorded from C127 cells and C1300 cells in the absence and presence of tamoxifen. Each column represents the mean \pm SEM (vertical bar).

dicating that Maxi-Cl-deficient C1300 cells are largely lacking in the SLCO2A1 expression. This fact is in complete agreement with our previous identification of SLCO2A1 as the core molecule for Maxi-Cl channel [8]. In addition, among 12 annexin A subfamilies, which are Ca²⁺-regulated membrane-binding proteins [23], ANXA1, ANXA2, ANXA3 and ANXA11 were previously shown to be expressed in the bleb membrane of C127 cells by LC-MS/MS proteomics [8], and here all these four members were found to be differentially less expressed in C1300 cells than in C127 cells with a signal ratio over two (Table 2). Since ANXA6 was previously suggested to be involved in upregulation of Maxi-Cl activity in placental syncytiotrophoblasts [24], we compared the levels of *Anxa6* expression between C127 cells and C1300 cells. The microarray analysis showed that *Anxa6* expression in C127 cells is not greater than that in C1300 cells with a C127/C1300 signal ratio of 0.86.

ANXA2 is involved in regulation of Maxi-Cl activity

ANXA2 is known to be a Ca²⁺- and actin-binding protein which is widely expressed in eukaryotic cells [for reviews see [25, 26]]. Also, ANXA2 was previously shown to be highly expressed in the bleb membrane derived from C127 cells with the emPA1 value of 7.33 [8]. Thus, we first observed the effects of siRNA-mediated knockdown of ANXA2 on Maxi-Cl activity (Fig. 2). This gene silencing was confirmed to efficiently downregulate expression of ANXA2 mRNA (*Anxa2*) and protein by RT-PCR (Fig. 2A) and western blotting (Fig. 2B), respectively. Maxi-Cl currents activated by membrane excision from C127 cells were never affected by pretreatment with non-targeting (negative control) siRNA (Fig. 2C) but prominently suppressed by *Anxa2* knockdown (Fig. 2D), as summarized for the data recorded at +25 mV in Fig. 2E. In contrast, siRNA-mediated knockdown either of *Anxa1*, *Anxa3* or *Anxa11* failed to affect Maxi-Cl currents in C127 cells (Supplementary Fig. 1), indicating that Maxi-Cl activity is regulated by the ANXA2 subfamily. Also, Maxi-Cl activity in swollen C127 cells treated with *Anxa6*-siRNA ($nP_o = 9.23 \pm 3.75$, n=5) was not significantly different from the cells treated with non-targeting siRNA ($nP_o = 9.63 \pm 3.47$, n=5; p>0.5). Furthermore, stable knockdown of *Anxa2* by microRNA (miRNA) was found to similarly suppress Maxi-Cl activity (Supplementary Fig. 2). In addition, as shown in Supplementary Fig. 3, Maxi-Cl activity was found to be sizably suppressed by the treatment with anti-ANXA2 monoclonal antibody for over 25 min (B, D) but not with control IgG (A, C). Gene silencing of *Anxa2* also markedly suppressed hypotonicity-induced ATP release from swollen C127 cells, which is known to

Table 1. List of genes of transmembrane proteins expressed in the bleb membrane of C127 cells and their differential expression in C1300 cells detected by microarray analysis

Symbol	Name	C127 signal	C1300 signal	C127/C1300 ratio
Slc15a4	solute carrier family 15, member 4	631	1071	0.6
Slc25a3	solute carrier family 25, member 3	10492	7923	1.3
Slc25a4	solute carrier family 25, member 4	6936	8635	0.8
Slc25a5	solute carrier family 25, member 5	6451	5656	1.1
Slc25a11	solute carrier family 25, member 11	3578	3855	0.9
Slc33a1	solute carrier family 33, member 1	457	186	2.5
Slc44a1	solute carrier family 44, member 1	3236	2776	1.2
Slc44a2	solute carrier family 44, member 2	1936	488	4.0
Slco2a1	solute carrier organic anion transporter family, member 2a1	4820	271	17.8
Tmem62	transmembrane protein 62	1446	443	3.3
Tmem65	transmembrane protein 65	1834	1493	1.2
Tmem97	transmembrane protein 97	1836	1972	0.9
Tmem167b	transmembrane protein 167B	1922	1520	1.3
Tmem189	transmembrane protein 189	3565	2552	1.4
Tspan31	tetraspanin 31	6866	7591	0.9

Table 2. List of genes of annexins expressed in the bleb membrane of C127 cells and their differential expression in C1300 cells detected by microarray analysis

Symbol	Name	C127 signal	C1300 signal	C127/C1300 ratio
Anxa1	annexin A1	6081	73	83.0
Anxa2	annexin A2	6430	917	7.0
Anxa3	annexin A3	3152	195	16.1
Anxa11	annexin A11	2385	654	3.6

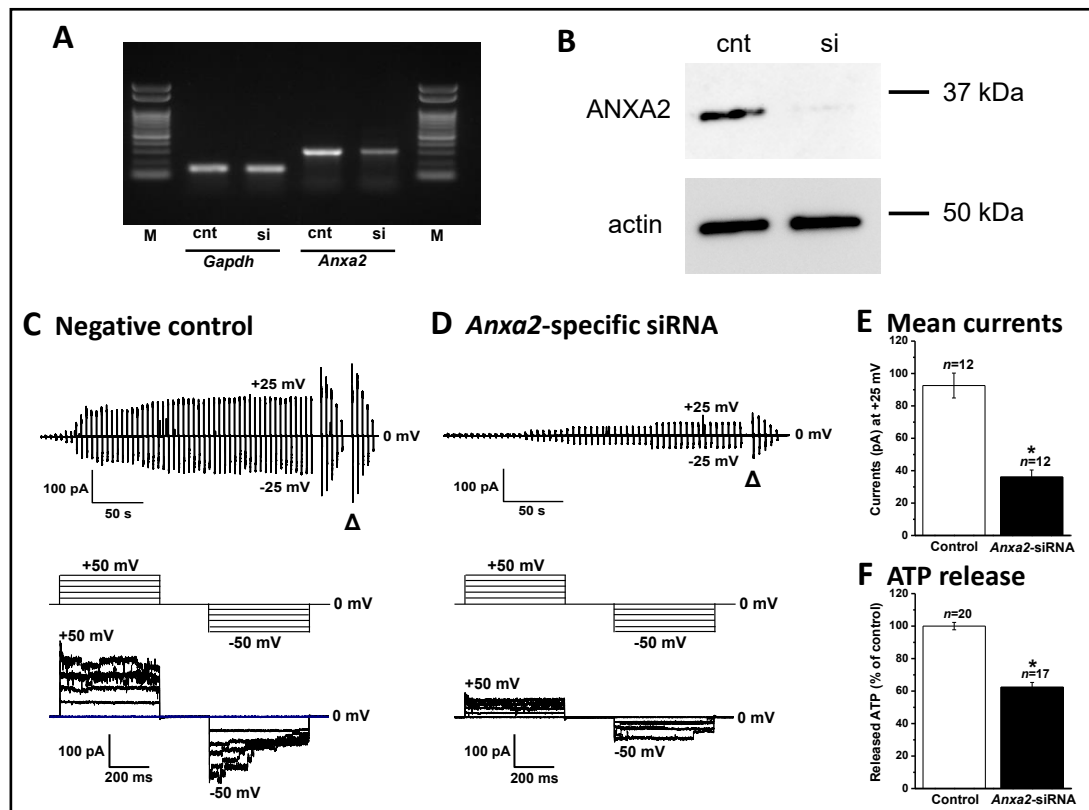


Fig. 2. Downregulation of Maxi-Cl activity by siRNA-mediated silencing of the expression of *Anxa2* in C127 cells. **A.** Expression of ANXA2 mRNA (*Anxa2*) in C127 cells treated with non-targeting siRNA (cnt) or *Anxa2*-specific siRNA (si) detected by RT-PCR using *Gapdh* as a control. M: molecular size markers (100-bp ladder). The data represent triplicate experiments. **B.** Expression of ANXA2 protein in C127 cells treated with non-targeting siRNA (cnt) or *Anxa2*-specific siRNA (si) assessed by western blotting using anti-ANXA2 antibody. Beta actin was detected as an internal control. Molecular weight markers (in kDa) are indicated on the right. The data represent triplicate experiments. **C, D.** The effects of transfection with non-targeting (Negative control) and *Anxa2*-specific siRNAs on Maxi-Cl activity. Top panels show the representative time courses of Maxi-Cl current activation after patch excision from C127 cells transfected with non-targeting siRNA (C) and *Anxa2*-specific siRNA (D). During the records, alternating pulses from 0 to ± 25 mV were applied. Bottom panels show the voltage-dependent inactivation pattern of Maxi-Cl currents elicited by applying voltage step pulses (500 ms) from 0 to ± 50 mV in 10-mV increments at the time points indicated by triangles in upper panels. The pulse protocol is shown in middle panels. **E, F.** Summary of the effects of non-targeting siRNA (Control) and *Anxa2*-specific siRNA on the mean Maxi-Cl currents recorded at +25 mV (E) and on hypotonicity-induced ATP release from swollen C127 cells (F). Each column represents the mean \pm SEM (vertical bar). * $p < 0.05$ (Student's t-test) vs Control.

be predominantly mediated by Maxi-Cl channels [6], as shown in Fig. 2F. Taken together, it is concluded that ANXA2 somehow regulates Maxi-Cl activity in an augmenting manner.

ANXA2 regulates Maxi-Cl activity via the interaction with SLCO2A1

We then studied possible colocalization of ANXA2 with SLCO2A1, the core component of Maxi-Cl channel, by immunostaining. As shown in Supplementary Fig. 3A, expression of endogenous ANXA2 was found to largely overlap with that of EGFP-tagged SLCO2A1 transfected in C127 cells, especially in the periphery region. To test a possibility of physical interaction between ANXA2 and SLCO2A1, we next conducted co-immunoprecipitation assay with using anti-FLAG antibody and anti-RFP polyclonal antibody (pAb) which recognizes DsRed. When *Slco2a1*-FLAG and *Anxa2*-DsRed2 were coexpressed in HEK293T cells, a co-immuno-

precipitated band was, in fact, observed, as shown in Supplementary Fig. 3B (left panel, at arrow). Reversely, when *Slco2a1*-EGFP and *Anxa2*-DsRed2 were coexpressed in HEK293T cells, SLCO2A1-EGFP was co-precipitated with ANXA2-DsRed2 which was immunoprecipitated with anti-ANXA2 antibody, as shown in Supplementary Fig. 3B (right panel, at arrow). Thus, there may be some physical interaction between ANXA2 and SLCO2A1 molecules.

We thus examined the effects of overexpression of *Anxa2* and *Slco2a1* in C1300 cells, which lack Maxi-Cl activity and ample SLCO2A1 expression, with using CMV-pIRES2-DsRed2 vector and/or CMV-pIRES2-EGFP vector. Heterologous overexpression of mouse *Anxa2-ires*-DsRed2 alone failed to elicit Maxi-Cl activity in C1300 cells (Fig. 3A). In contrast, two days after transfection with *Slco2a1-ires*-EGFP alone, membrane excision was found to induce activation of currents in C1300 cells (Fig. 3B). The currents exhibited sensitivity to bromosulphthalein (BSP: Fig. 3B-a) which was shown to block the Maxi-Cl current [8], and a unitary current amplitude of around 8.4 pA at -25 mV (Fig. 3B-b) which corresponds to a single-channel conductance of around 336 pS. Double overexpression of *Slco2a1-ires*-EGFP and *Anxa2-ires*-DsRed2 also induced Maxi-Cl activity in C1300 cells (Fig. 3C). As summarized in Fig. 3D, Maxi-Cl activity induced by double overexpression of SLCO2A1 and ANXA2 is significantly greater than that induced by single overexpression of SLCO2A1. These results show that ANXA2 per se cannot form the channel pore, but rather acts as a regulatory component for SLCO2A1/Maxi-Cl channel.

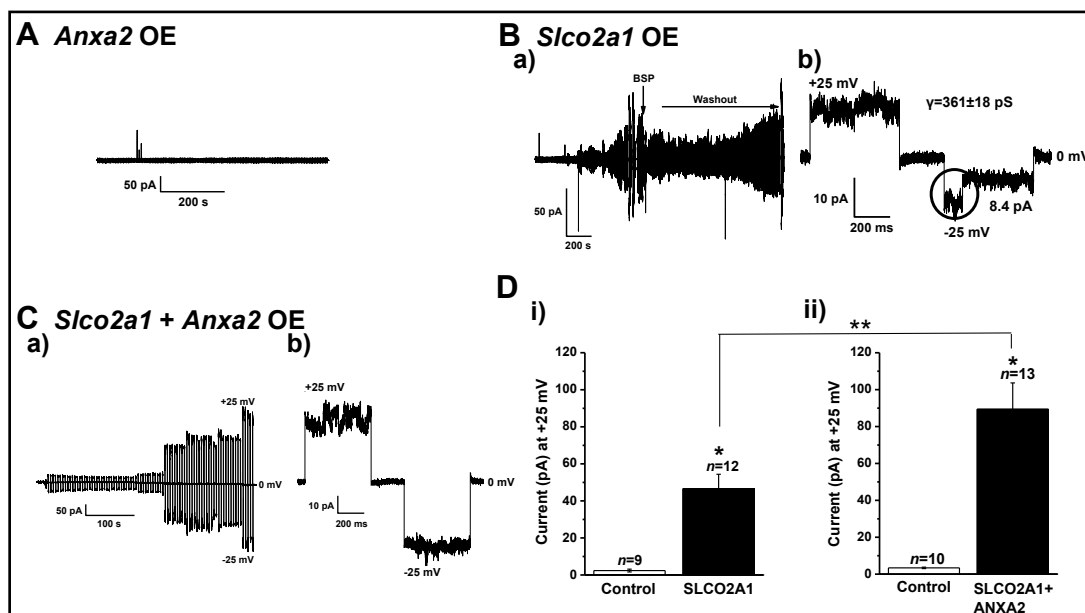


Fig. 3. Emergence of BSP-sensitive Maxi-Cl activity in C1300 cells by heterologous overexpression of *Slco2a1* alone or together with *Anxa2*. A, B, C. The effects of overexpression of ANXA2 alone, SLCO2A1 alone, and SLCO2A1 together with ANXA2 on Maxi-Cl activity. The currents were recorded after patch excision from C1300 cells during repetitive application (every 5 s) of alternating test pulses (± 25 mV for 0.5 s) from the holding potential (0 mV). Any Maxi-Cl activity was not observed in those transfected with *Anxa2* alone (A) ($n=7$). In contrast, Maxi-Cl currents were observed in C1300 cells transfected with *Slco2a1* alone (B) or together with *Anxa2* (C). These time courses of channel activation after patch excision during application of alternating pulses are shown in a, and single representative traces recorded upon a single alternating pulse are shown in b. The circle marks a representative single-channel event with a large amplitude (B-b). Effects of BSP (50 μ M) and washout of this drug are also shown in B-a. D. Summary of the effects of single overexpression of vector alone (Control) or SLCO2A1 alone (i) and double overexpression of vectors (Control) or SLCO2A1 plus ANXA2 (ii) on the mean Maxi-Cl currents recorded at +25 mV. Each column represents the mean \pm SEM (vertical bar). * $p<0.05$ (Student's t-test) vs Control. ** $p<0.05$ (Student's t-test) between the currents induced by double overexpression of SLCO2A1 plus ANXA2 and those induced by single overexpression SLCO2A1 alone.

ANXA2 confers tyrosine dephosphorylation dependence on Maxi-Cl activity

Activation of Maxi-Cl was shown to be induced by protein tyrosine dephosphorylation [16]. ANXA2 is known to be phosphorylated by protein tyrosine kinases, such as Src family and the insulin receptor, at the residue of Tyr23 [27-29]. Thus, we examined effects of overexpression of a phospho-mimicking ANXA2 mutant, *Anxa2*-Y23E, where Tyr23 is replaced with glutamic acid, on Maxi-Cl activity. When *Anxa2*-WT-DsRed2 was overexpressed in C127 cells, typical Maxi-Cl currents were activated upon patch membrane excision, as shown in Fig. 4A. In contrast, Maxi-Cl activity was found to be dramatically suppressed in the membrane patch excised from C127 cells transfected with *Anxa2*-Y23E-DsRed2 (Fig. 4B). These results and the data recorded at +25 mV summarized in Fig. 4C clearly indicate that tyrosine phosphorylation/dephosphorylation at Tyr23 of ANXA2 plays a critical role in inactivation/activation of Maxi-Cl channels.

ANXA2-S100A10 complex confers intracellular Ca²⁺ dependence on Maxi-Cl activity

ANXA2, which per se is a Ca²⁺-binding protein, is well known to form a heterotetrameric complex with S100A10 belonging to the Ca²⁺-binding S100 protein family [30], which is characterized by the presence of two consecutive EF-hand-type Ca²⁺-binding motifs [for reviews see [31, 32]]. Furthermore, the ANXA2-S100A10 complex has been reported to bind and regulate a number of types of ion channels [for reviews see [25, 32, 33]], including the volume-sensitive outwardly rectifying anion channel (VSOR) or volume-regulated anion channel (VRAC) [34] and the cAMP-activated CFTR anion channel [35-37]. In addition, the present microarray analysis showed that S100A10 is more profoundly expressed in C127 cells compared to C1300 cells with a signal ratio of 3.3. Thus, we examined effects of gene knockdown for *S100a10* on Maxi-Cl activity in C127 cells after confirming that *S100a10*-siRNA effectively downregulated expression of *S100a10* by RT-PCR (Fig. 5A). In fact, Maxi-Cl

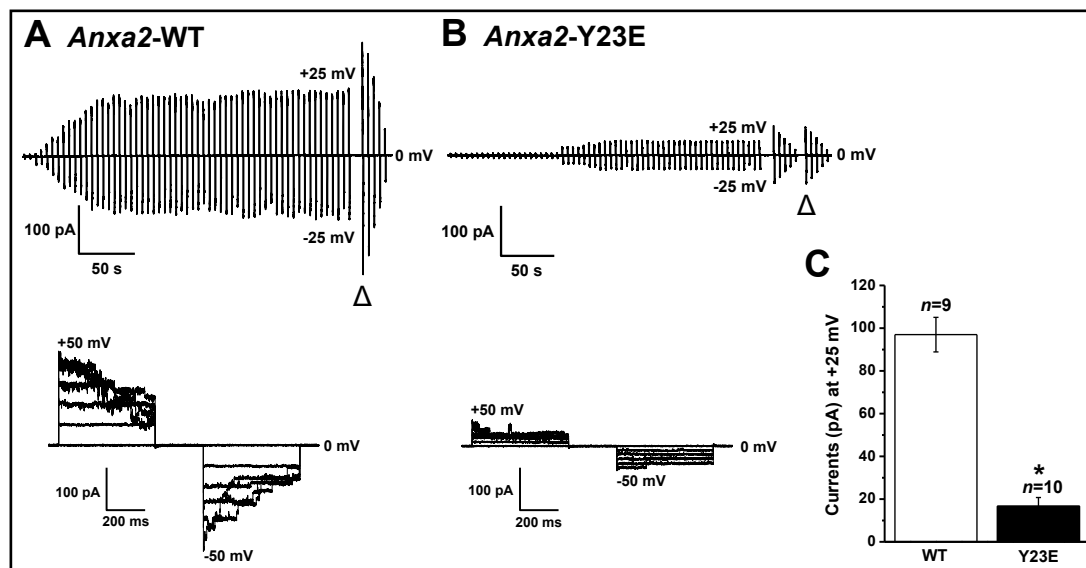


Fig. 4. Suppression of Maxi-Cl currents by overexpression of a phospho-mimicking ANXA2 mutant (ANXA2-Y23E) in C127 cells. A, B. The effects of overexpression of wild-type (WT) ANXA2 and ANXA2-Y23E on Maxi-Cl activity. Upper panels show the representative time courses of Maxi-Cl current activation after patch excision from the cells transfected with *Anxa2*-WT-DsRed2 as the control (A, top panel) and transfected with the phospho-mimicking mutant *Anxa2*-Y23E-DsRed2 (B, top panel). During the records, alternating pulses from 0 to ± 25 mV were applied. Bottom panels show the voltage-dependent inactivation pattern of Maxi-Cl currents elicited by applying voltage pulses (500 ms) from 0 to ± 50 mV in 10-mV increments at the time points indicated by triangles in upper panels. C. Summary of the effects of overexpression of wild-type ANXA2 (WT) and phospho-mimicking ANXA2-Y23E (Y23E) on Maxi-Cl currents recorded at +25 mV. Each column represents the mean \pm SEM (vertical bar). * $p < 0.05$ (Student's t-test) vs WT.

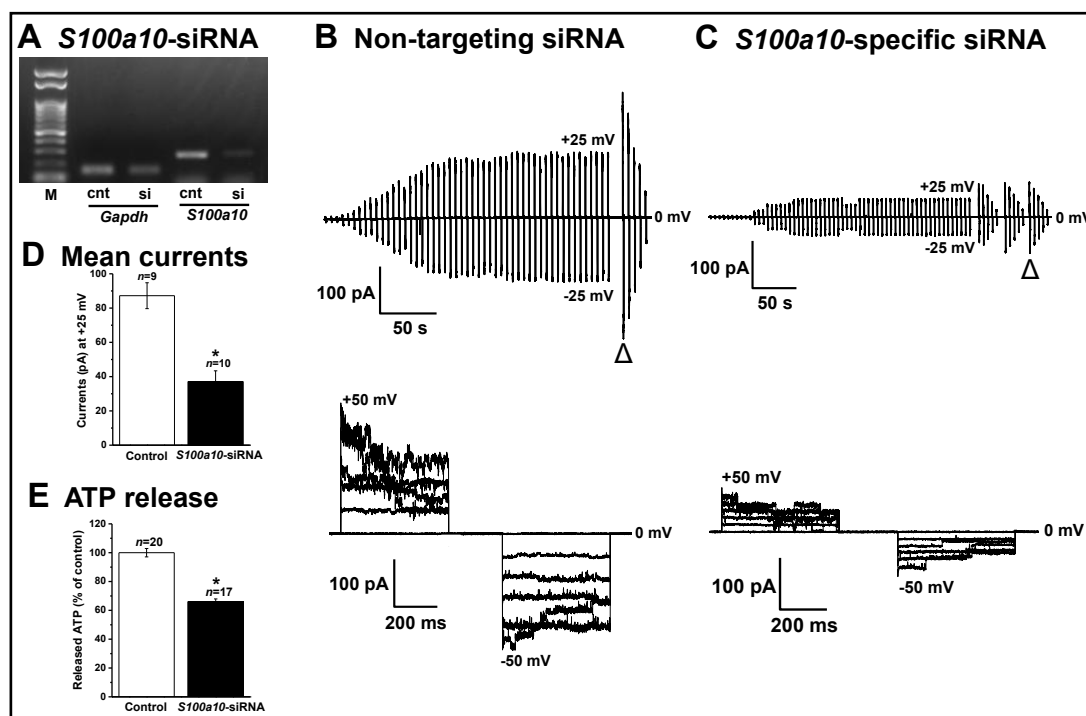


Fig. 5. Downregulation of Maxi-Cl activity by siRNA-mediated gene silencing of the expression of an obligate ANXA2 partner protein, S100A10, in C127 cells. **A.** RT-PCR analysis of expression of S100A10 mRNA (*S100a10*) in the cells transfected with non-targeting siRNA (cnt) or *S100a10*-specific siRNA (si). GAPDH mRNA (*Gapdh*) was used as an internal control. M: molecular size markers (100-bp ladder). The data represent quadruplicate experiments. **B, C.** The effects of transfection with non-targeting (negative control) and *S100a10*-specific siRNAs on Maxi-Cl activity. Upper panels show the representative time courses of Maxi-Cl current activation after patch excision from C127 cells transfected with non-targeting (negative control) siRNA (**B**) and *S100a10*-specific siRNA (**C**). During the records, alternating pulses from 0 to ± 25 mV were applied in the presence of 2 mM Ca^{2+} . Lower panels show the voltage-dependent inactivation pattern of Maxi-Cl currents elicited by applying step pulses (500 ms) from 0 to ± 50 mV in 10-mV increments at the time points indicated by triangles in upper panels. **D, E.** Summary of the effects of non-targeting siRNA (Control) and *S100a10*-specific siRNA on the mean Maxi-Cl currents recorded at +25 mV (**D**) and on hypotonicity-induced ATP release from C127 cells (**E**). Each column represents the mean \pm SEM (vertical bar). * $p < 0.05$ (Student's t-test) vs Control.

currents were largely suppressed by transfection of *S100a10*-specific siRNA (Fig. 5C and 5D), but not by that of non-targeting siRNA (Fig. 5B and 5D). Hypotonicity-induced ATP release from swollen C127 cells was also largely suppressed by *S100a10*-siRNA (Fig. 5E). Therefore, it appears that S100A10 is involved in the regulation of Maxi-Cl activity.

To test whether S100A10 exerts a regulatory action on Maxi-Cl via the complex formation with ANXA2, we next used a synthetic peptide consisting of the 14 N-terminal residues of ANXA2 with an acetylated N-terminal serine, Ac-(1-14), since this peptide interferes with the ANXA2-S100A10 complex formation by competing with endogenous ANXA2 for S100A10 binding [38]. When Ac-(1-14) was added only to the pipette (extracellular) solution, excision-activated Maxi-Cl currents (the mean currents recorded at +25 mV: 81.1 ± 11.0 pA, $n=9$) were not significantly different from those recorded in the absence of Ac-(1-14) (82.8 ± 7.2 pA, $n=9$; $p > 0.5$). As shown in Fig. 6, 100 μM Ac-(1-14) added to bathing (intracellular) solution prominently inhibited (**B**, left trace) or sometimes even abolished (**B**, right trace: $n=6$ of 12) excision-induced activation of Maxi-Cl in C127 cells (**C**: filled column). On the other hand, the negative control mutated peptide, L7E Ac-(1-14), which has a 1000 times lower affinity for ANXA2 [38], failed to affect Maxi-Cl activation (Fig. 6A and 6C: open

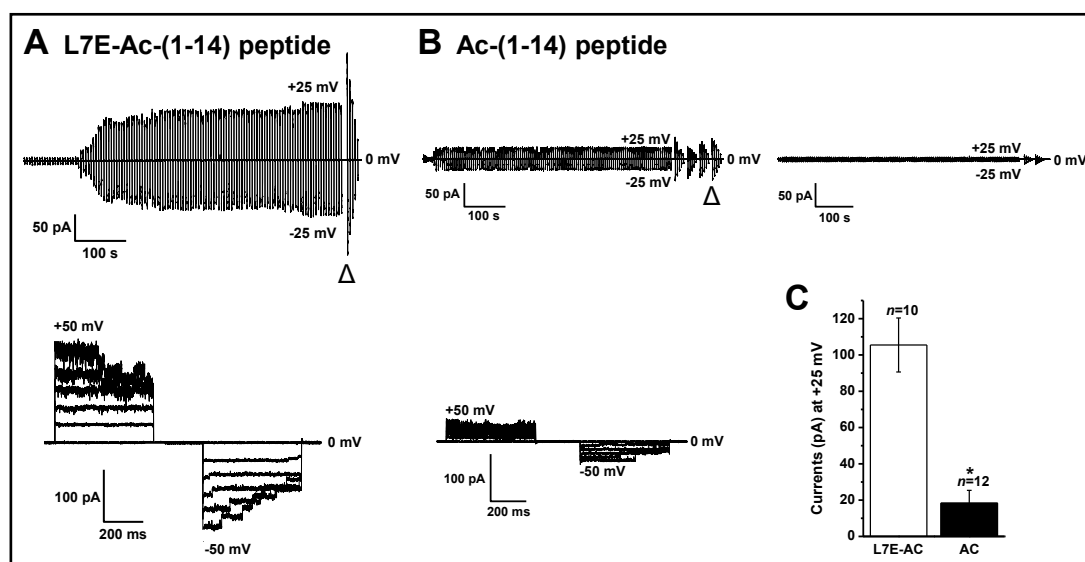


Fig. 6. Suppression of Maxi-Cl currents by a synthetic ANXA2 peptide, Ac-(1-14), but not by the mutated peptide, L7E Ac-(1-14), in C127 cells. A, B. The effects of intracellular application of synthetic ANXA2 and mutated peptides on Maxi-Cl activity. Upper panels show the representative time courses of activation of Maxi-Cl currents after patch excision from C127 cells treated with a mutated synthetic peptide, L7E Ac-(1-14), as negative control (A) and a synthetic ANXA2 peptide, Ac-(1-14) (B), which disrupts the ANXA2-S100A10 complex formation. Ac-(1-14) induced suppression (left: n=6 of 12) or abolition (right: n=6 of 12) of Maxi-Cl activity. During the records, alternating pulses from 0 to ± 25 mV were applied. Both peptides were added to bath (intracellular) solution before patch excision. Lower panels show the voltage-dependent inactivation pattern of Maxi-Cl currents elicited by applying voltage pulses (500 ms) from 0 to ± 50 mV in 10-mV increments at the time points indicated by triangles in upper panels. C. Summary of the effects of Ac-(1-14) (Ac) and its mutant (L7E-Ac) on Maxi-Cl currents recorded at +25 mV. Each column represents the mean \pm SEM (vertical bar). *p<0.05 (Student's t-test) vs L7E-Ac.

column). Thus, it is highly likely that S100A10-induced regulation of Maxi-Cl activity is mediated by the heteromeric complex formation between ANXA2 and S100A10.

Since the ANXA2-S100A10 complex is known to exhibit a higher affinity for Ca^{2+} than the ANXA2 monomer alone [39], we examined cytosolic Ca^{2+} dependence of Maxi-Cl activity. As shown in Fig. 7, Maxi-Cl channel activation after patch excision from C127 cells became more rapidly starting and more pronounced by intracellular free Ca^{2+} (A) in a manner dependent on the concentration in the range of 0.01 μM to 10 μM (B). However, even in the presence of 10 μM free Ca^{2+} , as also shown in Fig. 7, Maxi-Cl activity was remarkably suppressed by siRNA-mediated knockdown of *S100a10* in C127 cells (D, G), whereas Maxi-Cl activity was not affected by negative control mock-siRNA transfection (C, G). In contrast, excision-induced Maxi-Cl activation in C127 cells transfected not only with *S100a10*-siRNA but also with mock-siRNA was virtually abolished by reducing the intracellular free Ca^{2+} concentration down to 0.01 μM (Fig. 7E, 7F and 7G). Taken together, it is concluded that the ANXA2-S100A10 complex confers intracellular Ca^{2+} sensitivity on Maxi-Cl channels.

Discussion

Maxi-Cl represents the major type of large-conductance anion channels or maxi-anion channels (MACs) and plays essential roles in inorganic anion transport, cell volume regulation and release of ATP and glutamate not only in physiological processes but also in pathological processes especially during ischemia- or ischemia/reperfusion-induced injury in the brain and heart [for reviews see [1, 3, 9, 40]]. Although the phenotypical properties of

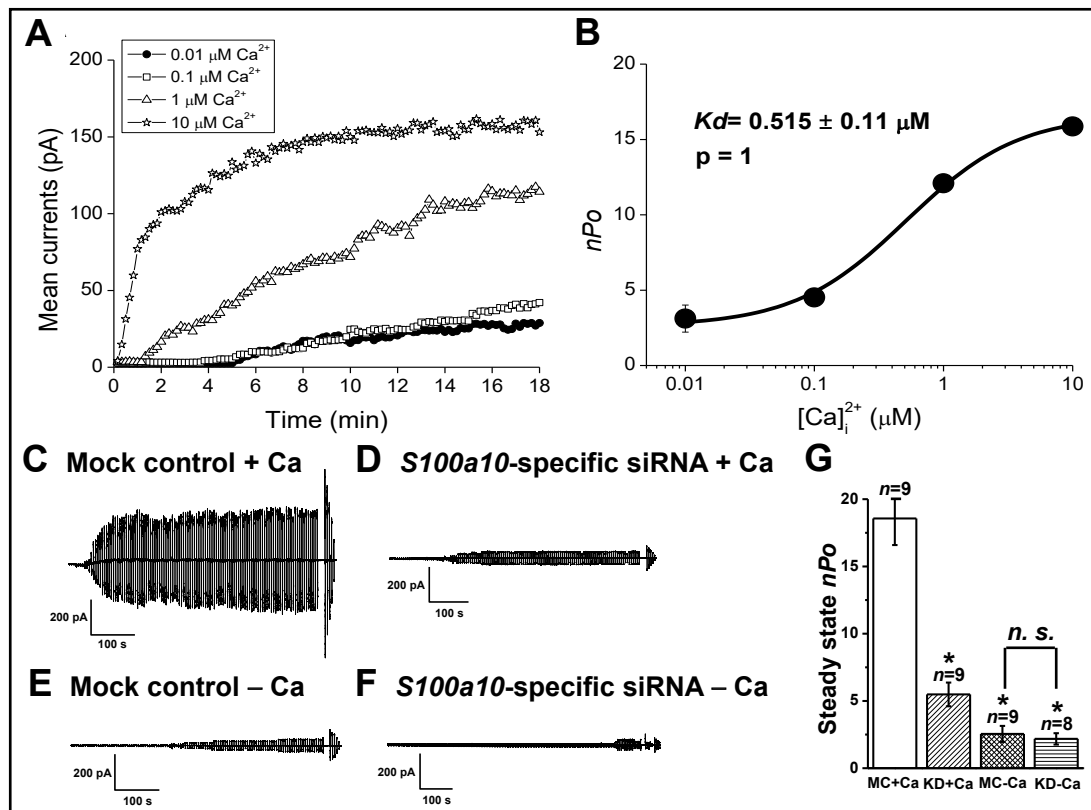


Fig. 7. Intracellular Ca^{2+} sensitivity of Maxi-Cl currents and its inhibition by knockdown of *S100a10* in C127 cells. **A.** Time courses of Maxi-Cl channel activation after patch excision from C127 cells recorded at +25 mV under conditions in which the intracellular side of patch membrane was exposed to AIs containing free Ca^{2+} at given concentrations ($n=5-7$). **B.** Concentration-dependent activation of Maxi-Cl channels by intracellular free Ca^{2+} . The nPo (mean number of channels open) values are plotted as a function of free Ca^{2+} concentration. Each circle point represents the mean \pm SEM (vertical bar). **C, D, E, F.** Representative time courses of Maxi-Cl current activation after patch excision from C127 cells transfected with non-targeting (Mock control) siRNA (**C, E**) and *S100a10*-specific siRNA (**D, F**). During these records, alternating pulses from 0 to ± 25 mV were applied in the presence (+Ca: **C, D**) or absence (-Ca: **E, F**) of 10 μM free Ca^{2+} . **G.** Summary of the effects of $\pm 10 \mu\text{M}$ free Ca^{2+} for the mock control (MC) and *S100a10*-specific siRNA knockdown (KD) on the steady-state nPo value recorded at +25 mV. Each column represents the mean \pm SEM (vertical bar). * $p < 0.05$ (ANOVA) vs MC+Ca.

Maxi-Cl have been well defined [for reviews see [1, 2, 41]], the molecular identity was not uncovered for over three decades since the discovery of Maxi-Cl currents [42]. In 2017, we eventually identified a member of solute carrier organic anion transporter family member, SLCO2A1, as the core component molecule for Maxi-Cl by applying proteomics and unbiased genome-wide approaches [8]. Maxi-Cl is normally in the non-activated state in intact cells without any stimulation [6, 9]. In contrast, the channel reconstituted from recombinant SLCO2A1 proteins was constitutively activated [8]. These facts indicate that the whole Maxi-Cl complex contains not only the core component SLCO2A1 but also some other component involved in the channel activation mechanism which has been remained elusive [for review see [9]].

Annexins comprise a large superfamily of Ca^{2+} -dependent, phospholipid-binding proteins [23, 25] and are expressed in vertebrates (ANXA), invertebrates (ANXB), fungi and protozoa (ANXC), plants (ANXD), and protists (ANXE) [33, 43]. Among 12 vertebrate annexin subfamilies (ANXA1 to ANXA11 and ANXA13), ANXA2 has been shown to play key roles in diverse membrane-related cell functions and to link F-actin cytoskeleton to the plasma

membrane [44]. Our previous LC-MS/MS proteomics study [8] showed that ANXA2 is most prominently expressed in the bleb membrane of Maxi-Cl-rich C127 cells. In addition, in the present study, not only SLCO2A1 but also ANXA2 were found to be differentially less expressed in Maxi-Cl-deficient C1300 cells by microarray analysis (Table 1 and Supplementary Table 1). In Maxi-Cl-rich C127 cells, a considerable part of ANXA2 was found to be colocalized with SLCO2A1 especially in the periphery region of the cells (Supplementary Fig. 3A). Furthermore, co-immunoprecipitation assay suggested some physical interaction between ANXA2 and SLCO2A1 (Supplementary Fig. 3B). These data raise a possibility that ANXA2 exerts a regulatory action to Maxi-Cl/SLCO2A1 channels. This inference was, in fact, verified by the following three lines of evidence. First, gene silencing of ANXA2 largely suppressed Maxi-Cl currents in and swelling-induced ATP release from C127 cells (Fig. 2D, 2E and 2F). Second, Maxi-Cl activity was partially suppressed by exposure of C127 cells to anti-ANXA2 monoclonal antibody (Supplementary Fig. 4). Third, Maxi-Cl activity elicited by overexpression of SLCO2A1 in C1300 cells became enhanced by simultaneous overexpression of ANXA2 (Fig. 3C and 3D).

In addition to ANXA2, three other vertebrate annexin subfamilies, ANXA1, ANXA3 and ANXA11, that were previously shown to be expressed in the bleb membrane of C127 cells [8], were also found to be less expressed in C1300 cells compared to in C127 cells (Table 2). However, siRNA-mediated knockdown of either ANXA1, ANXA3 or ANXA11 failed to affect MaxiCl activity in C127 cells (Supplementary Fig. 1). ANXA6 was suggested to be involved in upregulation of Maxi-Cl activity in placental syncytiotrophoblasts on the basis of the suppressive effect of anti-ANXA6 antibody [24]. However, our previous LC-MS/MS proteomics study [8] showed that ANXA6 expression in the bleb membrane of C127 cells was not significant. Furthermore, the present microarray analysis showed that the *Anxa6* expression level in Maxi-Cl-rich C127 cells is not higher than that in Maxi-Cl-deficient C1300 cells. Also, the present electrophysiological study demonstrated that Maxi-Cl activity in C127 cells was not affected by treatment with *Anxa6*-siRNA. Thus, in the present study, possible involvements of other annexin subfamilies in Maxi-Cl regulation were not supported, though not be firmly ruled out. In contrast, it is evident that ANXA2 plays a regulatory role in Maxi-Cl activity.

A number of annexins form complexes with specific members of S100 protein family which possesses two consecutive EF-hand type Ca^{2+} -binding motifs. ANXA2 forms a heterotetramer with its obligated partner S100 protein, S100A10 also called an annexin light chain, consisting of an S100A dimer sandwiched between two ANXA2 proteins [for review see [31]], the first 14 N-terminal residues of which provide the S100A10-binding site [45]. In the present study, S100A10 was found to be less expressed in C1300 cells by microarray assay in comparison with C127 cells. Also, siRNA-mediated *S100a10* silencing was shown to suppress Maxi-Cl currents and swelling-induced ATP release from C127 cells (Fig. 5). Thus, it appears that S100A10 is also involved in regulation of Maxi-Cl activity. This S100A10 action is mediated through the interaction with ANXA2, since excision-induced activation of Maxi-Cl in C127 cells was largely inhibited by application of a synthetic peptide consisting of the first 14 N-terminal residues of ANXA2 with an acetylated N-terminal serine, Ac-(1-14), which disrupts the formation of ANXA2-S100A10 complex [38], but not by that of its mutated negative control peptide, L7E Ac-(1-14) (Fig. 6).

The ANXA2-S100A10 complex is involved in a large variety of physiological/pathophysiological processes by interacting with many types of target molecules including phospholipids, cytoskeletons, receptors, enzymes, transporters and ion channels [for reviews see [25, 32, 33]]. Previous studies have accumulated evidence for ANXA2-S100A10 complex-mediated regulation of activity or translocation of multiple types of ion channels, including K^+ channels such as TASK-1 [46, 47], Na^+ channels such as $\text{Na}_v1.8$ [48, 49], ENaC [50] and ASIC1a [51], and cation channels such as TRPA1 [52] and TRPV4/5/6 [53-56] as well as anion channels such as VSOR/VRAC [34] and CFTR [35-37]. The present study added Maxi-Cl as a new example of ion channel regulated by ANXA2-S100A10 complex.

In the present study, the mechanisms of regulation of Maxi-Cl by ANXA2-S100A10 complex were also elucidated. Maxi-Cl activity is basally inactivated in the unstimulated intact

cells. Maxi-Cl activation was shown to be induced by maneuvers to induce protein tyrosine dephosphorylation even in the on-cell or cell-attached configuration [16]. However, its molecular basis has not been known. ANXA2 is known to be phosphorylated by protein tyrosine kinase at Tyr23 of its N-terminal domain [27-29]. This fact raises a possibility that tyrosine dephosphorylation-induced Maxi-Cl activation is mediated by Tyr23 of ANXA2. In fact, overexpression of a phospho-mimicking ANXA2 mutant, *Anxa2-Y23E*, prominently inhibited excision-induced Maxi-Cl activation in C127 cells (Fig. 4). Maxi-Cl activity in the cell-attached patch membranes was shown to become activated by application of a Ca^{2+} ionophore [11, 12, 14, 15]. Thus, it has been deemed that an increase in the intracellular free Ca^{2+} concentration may activate Maxi-Cl channels. In the present study, actually, Maxi-Cl activity was demonstrated to be activated by an increase in the intracellular free Ca^{2+} level in a concentration-dependent manner (Fig. 7A and 7B). ANXA2 is a Ca^{2+} -binding protein with containing non-EF-hand-type Ca^{2+} -binding sites at the C-terminal core [for review see [37]]. Moreover, the ANXA2-S100A10 complex has a higher Ca^{2+} affinity than ANXA2 monomer alone [39]. These facts may suggest that the ANXA2-S100A10 complex is directly involved in intracellular Ca^{2+} dependence of Maxi-Cl activity. In fact, siRNA-mediated knockdown of *S100a10* virtually abolished Ca^{2+} dependence of Maxi-Cl activity in C127 cells (Fig. 7D and 7G). On balance, it can be concluded that dependence of Maxi-Cl activity not only on intracellular free Ca^{2+} rise but also on protein tyrosine dephosphorylation are conferred by the ANXA2-S100A10 complex with directly interacting with its core molecule, SLCO2A1.

Ischemic and hypotonic stress was shown to activate Maxi-Cl currents in isolated astrocytes thereby inducing release of glutamate [57] and ATP [21, 58]. Oxygen-glucose deprivation was also shown to activate single-channel events of Maxi-Cl in the cell-attached patch membrane on astrocytes in the brain slice [3]. Activation of Maxi-Cl currents was also induced by hypotonic and ischemic stress in isolated ventricular myocytes [59, 60], thereby causing ATP release from these cells [60]. Ischemia-reperfusion insult was also observed to induce ATP release in Langendorff-perfused hearts of adult mice in a manner sensitive to *in vivo* gene silencing of the Maxi-Cl core molecule, SLCO2A1 [8]. Since ischemia/hypoxia stress was shown to promote the interaction of ANXA2-S100A10 complex with the plasma membrane [61], there is a possibility that ischemia/hypoxia-induced activation of Maxi-Cl channels is mediated by increased interaction between the ANXA2-S100A10 complex and SLCO2A1 integrated in the plasma membrane. In any case, targeting the Maxi-Cl core component SLCO2A1 and its regulatory component ANXA2-S100A10 complex may have potential therapeutic benefits for ischemia/hypoxia-induced injury in the brain and heart.

Conclusion

In the present study, identification of SLCO2A1 as the Maxi-Cl core component was verified by the following two observations. First, SLCO2A1 was found to be markedly less expressed in Maxi-Cl-deficient C1300 cells (Table 1). Second, SLCO2A1 overexpression was shown to elicit Maxi-Cl activity from endogenously Maxi-Cl activity-lacking C1300 cells (Fig. 3B and 3D). Moreover, in the present study, we identified the ANXA2-S100A10 complex as Maxi-Cl/SLCO2A1 channel's regulatory component conferring protein tyrosine dephosphorylation dependence and intracellular free Ca^{2+} sensitivity on this channel. These regulatory actions of ANXA2-S100A10 may well explain why Maxi-Cl/SLCO2A1 channel is activated in intact cells by maneuvers to induce protein tyrosine dephosphorylation or to increase the intracellular free Ca^{2+} concentration. These ANXA2-S100A10 actions may also be causatively involved in activation of Maxi-Cl/SLCO2A1 channel and ATP release in the brain and heart under ATP-depleting ischemic situations.

Acknowledgements

We thank K Shigemoto for her technical assistance. This work was supported by Grants-in-Aid for Scientific Research from JSPS of Japan to YO (#17K19517) and TO (#16K08510). MRI was supported by 'JSPS Postdoctoral Fellowship' for the foreign researchers. MRI, PGM and RZS have received 'NIPS Invited Scientist' fellowship from the National Institute for Physiological Sciences (NIPS), Okazaki, Japan.

YO and RZS conceived of the project and its design; MRI, TO, PGM, AHT and YA-A performed experiments and data analysis; MRI prepared figures and drafted the manuscript; YO edited and revised manuscript; RZS and TO commented on the manuscript; and YO approved final version of the manuscript.

Disclosure Statement

The authors have no conflicts of interest to declare.

References

- 1 Sabirov RZ, Merzlyak PG, Islam MR, Okada T, Okada Y: The properties, functions and pathophysiology of maxi-anion channels. *Pflugers Arch* 2016;468:405-420.
- 2 Okada Y, Okada T, Sato-Numata K, Islam MR, Ando-Akatsuka Y, Numata T, Kubo M, Shimizu T, Kurbannazarova RS, Marunaka Y, Sabirov RZ: Cell volume-activated and volume-correlated anion channels in mammalian cells: their biophysical, molecular, and pharmacological properties. *Pharmacol Rev* 2019;71:49-88.
- 3 Okada Y, Numata T, Sato-Numata K, Sabirov RZ, Liu H, Mori SI, Morishima S: Roles of volume-regulatory anion channels, VSOR and Maxi-Cl, in apoptosis, cisplatin resistance, necrosis, ischemic cell death, stroke and myocardial infarction. *Curr Top Membr* 2019;83:205-283.
- 4 Georgi MI, Rosendahl J, Ernst F, Günzel D, Aschenbach JR, Martens H, Stumpff F: Epithelia of the ovine and bovine forestomach express basolateral maxi-anion channels permeable to the anions of short-chain fatty acids. *Pflugers Arch* 2014;466:1689-1712.
- 5 Stumpff F: A look at the smelly side of physiology: transport of short chain fatty acids. *Pflugers Arch* 2018;470:571-598.
- 6 Sabirov RZ, Dutta AK, Okada Y: Volume-dependent ATP-conductive large-conductance anion channel as a pathway for swelling-induced ATP release. *J Gen Physiol* 2001;118:251-266.
- 7 Sabirov RZ, Okada Y: ATP release via anion channels. *Purinergic Signal* 2005;1:311-328.
- 8 Sabirov RZ, Merzlyak PG, Okada T, Islam MR, Uramoto H, Mori T, Makino Y, Matsuura H, Xie Y, Okada Y: The organic anion transporter SLC02A1 constitutes the core component of the Maxi-Cl channel. *EMBO J* 2017;36:3309-3324.
- 9 Okada Y, Okada T, Islam MR, Sabirov RZ: Molecular identities and ATP release activities of two types of volume-regulatory anion channels, VSOR and Maxi-Cl. *Curr Top Membr* 2018;81:125-176.
- 10 Hoffmann EK, Lambert IH, Pedersen SF: Physiology of cell volume regulation in vertebrates. *Physiol Rev* 2009;89:193-277.
- 11 Light DB, Schwiebert EM, Fejes-Toth G, Naray-Fejes-Toth A, Karlson KH, McCann FV, Stanton BA: Chloride channels in the apical membrane of cortical collecting duct cells. *Am J Physiol* 1990;258:F273-F280.
- 12 Kawahara K, Takuwa N: Bombesin activates large-conductance chloride channels in Swiss 3T3 fibroblasts. *Biochem Biophys Res Commun* 1991;177:292-298.
- 13 Groschner K, Kukovetz WR: Voltage-sensitive chloride channels of large conductance in the membrane of pig aortic endothelial cells. *Pflugers Arch* 1992;421:209-217.
- 14 Bajnath RB, Groot JA, de Jonge HR, Kansen M, Bijman J: Calcium ionophore plus excision induce a large conductance chloride channel in membrane patches of human colon carcinoma cells HT-29cl.19A. *Experientia* 1993;49:313-316.

- 15 Sun XP, Supplisson S, Mayer E: Chloride channels in myocytes from rabbit colon are regulated by a pertussis toxin-sensitive G protein. *Am J Physiol* 1993;264:G774-G785.
- 16 Toychiev AH, Sabirov RZ, Takahashi N, Ando-Akatsuka Y, Liu H, Shintani T, Noda M, Okada Y: Activation of maxi-anion channel by protein tyrosine dephosphorylation. *Am J Physiol Cell Physiol* 2009;297:C990-C1000.
- 17 Islam MR, Uramoto H, Okada T, Sabirov RZ, Okada Y: Maxi-anion channel and pannexin 1 hemichannel constitute separate pathways for swelling-induced ATP release in murine L929 fibrosarcoma cells. *Am J Physiol Cell Physiol* 2012;303:C924-C935.
- 18 Ikebuchi NW, Waisman DM: Calcium-dependent regulation of actin filament bundling by lipocortin-85. *J Biol Chem* 1990;265:3392-3400.
- 19 Jones PG, Moore GJ, Waisman DM: A nonapeptide to the putative F-actin binding site of annexin-II tetramer inhibits its calcium-dependent activation of actin filament bundling. *J Biol Chem* 1992;267:13993-13997.
- 20 Hayes MJ, Shao D, Bailly M, Moss SE: Regulation of actin dynamics by annexin 2. *EMBO J* 2006;25:1816-1826.
- 21 Liu HT, Toychiev AH, Takahashi N, Sabirov RZ, Okada Y: Maxi-anion channel as a candidate pathway for osmosensitive ATP release from mouse astrocytes in primary culture. *Cell Res* 2008;18:558-565.
- 22 Díaz M, Bahamonde MI, Lock H, Muñoz FJ, Hardy SP, Posas F, Valverde MA: Okadaic acid-sensitive activation of Maxi Cl⁻ channels by triphenylethylene antioestrogens in C1300 mouse neuroblastoma cells. *J Physiol* 2001;536:79-88.
- 23 Gerke V, Creutz CE, Moss SE: Annexins: linking Ca²⁺ signaling to membrane dynamics. *Nat Rev Mol Cell Biol* 2005;6:449-461.
- 24 Riquelme G, Llanos P, Tischner E, Neil J, Campos B: Annexin 6 modulates the maxi-chloride channel of the apical membrane of syncytiotrophoblast isolated from human placenta. *J Biol Chem* 2004;279:50601-50608.
- 25 Gerke V, Moss SE: Annexins: from structure to function. *Physiol Rev* 2002;82:331-371.
- 26 Grieve AG, Moss SE, Hayes MJ: Annexin A2 at the interface of actin and membrane dynamics: a focus on its roles in endocytosis and cell polarization. *Int J Cell Biol* 2012;2012:852430.
- 27 Glenney JR Jr, Tack BF: Amino-terminal sequence of p36 and associated p10: identification of the site of tyrosine phosphorylation and homology with S-100. *Proc Natl Acad Sci USA* 1985;82:7884-7888.
- 28 Gould KL, Woodgett JR, Isacke CM, Hunter T: The protein-tyrosine kinase substrate p36 is also a substrate for protein kinase C *in vitro* and *in vivo*. *Mol Cell Biol* 1986;6:2738-2744.
- 29 Karasik A, Pepinsky RB, Kahn CR: Insulin and epidermal growth factor stimulate phosphorylation of a 170-kDa protein in intact hepatocytes immunologically related to lipocortin 1. *J Biol Chem* 1988;263:18558-18562.
- 30 Santamaria-Kisiel L, Rintala-Dempsey AC, Shaw GS: Calcium-dependent and -independent interactions of the S100 protein family. *Biochem J* 2006;396:201-214.
- 31 Rescher U, Gerke V: S100A10/p11: family, friends and functions. *Pflugers Arch* 2008;455:575-582.
- 32 Madureira PA, O'Connell PA, Surette AP, Miller VA, Waisman DM: The biochemistry and regulation of S100A10: a multifunctional plasminogen receptor involved in oncogenesis. *J Biomed Biotechnol* 2012;2012:353687.
- 33 Lizarbe MA, Barrasa JI, Olmo N, Gavilanes F, Turnay J: Annexin-phospholipid interactions. Functional implications. *Int J Mol Sci* 2013;14:2652-2683.
- 34 Nilius B, Gerke V, Prenen J, Szücs G, Heinke S, Weber K, Droogmans G: Annexin II modulates volume-activated chloride currents in vascular endothelial cells. *J Biol Chem* 1996;271:30631-30636.
- 35 Borthwick LA, McGaw J, Conner G, Taylor CJ, Gerke V, Mehta A, Robson L, Muimo R: The formation of the cAMP/protein kinase A-dependent annexin 2-S100A10 complex with cystic fibrosis conductance regulator protein (CFTR) regulates CFTR channel function. *Mol Biol Cell* 2007;18:3388-3397.
- 36 Borthwick LA, Riemen C, Goddard C, Colledge WH, Mehta A, Gerke V, Muimo R: Defective formation of PKA/CnA-dependent annexin 2-S100A10/CFTR complex in ΔF508 cystic fibrosis cells. *Cell Signal* 2008;20:1073-1083.
- 37 Muimo R: Regulation of CFTR function by annexin A2-S100A10 complex in health and disease. *Gen Physiol Biophys* 2009;28:F14-F19.
- 38 Becker T, Weber K, Johnsson N: Protein-protein recognition via short amphiphilic helices; a mutational analysis of the binding site of annexin II for p11. *EMBO J* 1990;9:4207-4213.

- 39 Powell MA, Glenney JR: Regulation of calpactin I phospholipid binding by calpactin I light-chain binding and phosphorylation by p60v-src. *Biochem J* 1987;247:321-328.
- 40 Sabirov RZ, Okada Y: The maxi-anion channel: a classical channel playing novel roles through an unidentified molecular entity. *J Physiol Sci* 2009;59:3-21.
- 41 Sabirov RZ, Merzlyak PG: Plasmalemmal VDAC controversies and maxi-anion channel puzzle. *Biochim Biophys Acta* 2012;1818:1570-1580.
- 42 Blatz AL, Magleby KL: Single voltage-dependent chloride-selective channels of large conductance in cultured rat muscle. *Biophys J* 1983;43:237-241.
- 43 Hoque M, Rentero C, Cairns R, Tebar F, Enrich C, Grewal T: Annexins - scaffolds modulating PKC localization and signaling. *Cell Signal* 2014;26:1213-1225.
- 44 Bharadwaj A, Bydoun M, Holloway R, Waisman D: Annexin A2 heterotetramer: structure and function. *Int J Mol Sci* 2013;14:6259-6305.
- 45 Kube E, Becker T, Weber K, Gerke V: Protein-protein interaction studied by site-directed mutagenesis. Characterization of the annexin II-binding site on p11, a member of the S100 protein family. *J Biol Chem* 1992;267:14175-14182.
- 46 Girard C, Tinel N, Terrenoire C, Romey G, Lazdunski M, Borsotto M: p11, an annexin II subunit, an auxiliary protein associated with the background K⁺ channel, TASK-1. *EMBO J* 2002;21:4439-4448.
- 47 Renigunta V, Yuan H, Zuzarte M, Rinné S, Koch A, Wischmeyer E, Schlichthörl G, Gao Y, Karschin A, Jacob R, Schwappach B, Daut J, Preisig-Müller R: The retention factor p11 confers an endoplasmic reticulum-localization signal to the potassium channel TASK-1. *Traffic* 2006;7:168-181.
- 48 Okuse K, Malik-Hall M, Baker MD, Poon WY, Kong H, Chao MV, Wood JN: Annexin II light chain regulates sensory neuron-specific sodium channel expression. *Nature* 2006;417:653-656.
- 49 Poon WY, Malik-Hall M, Wood JN, Okuse K: Identification of binding domains in the sodium channel Na(V)1.8 intracellular N-terminal region and annexin II light chain p11. *FEBS Lett* 2004;58:114-118.
- 50 Cheung TT, Ismail NAS, Moir R, Arora N, McDonald FJ, Condliffe SB: Annexin II light chain p11 interacts with ENaC to increase functional activity at the membrane. *Front Physiol* 2019;10:7.
- 51 Donier E, Rugiero F, Okuse K, Wood JN: Annexin II light chain p11 promotes functional expression of acid-sensing ion channel ASIC1a. *J Biol Chem* 2005;280:8666-38672.
- 52 Avenali L, Narayanan P, Rouwette T, Cervellini I, Sereda M, Gomez-Varela D, Schmidt M: Annexin A2 regulates TRPA1-dependent nociception. *J Neurosci* 2014;34:14506-14516.
- 53 van de Graaf SF, Hoenderop JG, Gkika D, Lamers D, Prenen J, Rescher U, Gerke V, Staub O, Nilius B, Bindels RJ: Functional expression of the epithelial Ca²⁺ channels (TRPV5 and TRPV6) requires association of the S100A10-annexin 2 complex. *EMBO J* 2003;22:1478-1487.
- 54 Borthwick LA, Neal A, Hobson L, Gerke V, Robson L, Muimo R: The annexin 2-S100A10 complex and its association with TRPV6 is regulated by cAMP/PKA/CnA in airway and gut epithelia. *Cell Calcium* 2008;44:147-157.
- 55 Huai J, Zhang Y, Liu QM, Ge HY, Arendt-Nielsen L, Jiang H, Yue SW: Interaction of transient receptor potential vanilloid 4 with annexin A2 and tubulin beta 5. *Neurosci Lett* 2012;512:22-27.
- 56 Ning L, Wang C, Ding X, Zhang Y, Wang X, Yue S: Functional interaction of TRPV4 channel protein with annexin A2 in DRG. *Neurol Res* 2012;34:685-693.
- 57 Liu HT, Tashmukhamedov BA, Inoue H, Okada Y, Sabirov RZ: Roles of two types of anion channels in glutamate release from mouse astrocytes under ischemic or osmotic stress. *Glia* 2006;54:343-357.
- 58 Liu HT, Sabirov RZ, Okada Y: Oxygen-glucose deprivation induces ATP release via maxi-anion channels in astrocytes. *Purinergic Signal* 2008;4:147-154.
- 59 Coulombe A, Coraboef E: Large-conductance chloride channels of new-born rat cardiac myocytes are activated by hypotonic media. *Pflugers Arch* 1992;422:143-150.
- 60 Dutta AK, Sabirov RZ, Uramoto H, Okada Y: Role of ATP-conductive anion channel in ATP release from neonatal rat cardiomyocytes in ischaemic or hypoxic conditions. *J Physiol* 2004;559:799-812.
- 61 Monastyrskaya K, Tschumi F, Babychuk EB, Stroka D, Draeger A: Annexins sense changes in intracellular pH during hypoxia. *Biochem J* 2008;409:65-75.